Appl. Phys. B 88, 433–442 (2007)
DOI: 10.1007/s00340-007-2718-3

Applied Physics B
Lasers and Optics

O.A. BURYY[1,✉]
D.Y. SUGAK[2]
S.B. UBIZSKII[1]
I.I. IZHNIN[2]
M.M. VAKIV[2]
I.M. SOLSKII[2]

The comparative analysis and optimization of the free-running Tm^{3+}:YAP and Tm^{3+}:YAG microlasers

[1] Institute of Telecommunications, Radioelectronics and Electronic Engineering, Lviv Polytechnic National University, Bandery St. 12, Lviv 79046, Ukraine
[2] Institute of Materials, SRC "Carat", Stryjska St. 202, Lviv 79031, Ukraine

Received: 14 December 2006 / Revised version: 12 April 2007
Published online: 12 July 2007 •

ABSTRACT The thulium microlasers based on yttrium-aluminium perovskite and yttrium-aluminium garnet crystals are considered as coherent light sources at the wavelength near 2 μm. The comparative analysis of these lasers is carried out by means of the lasers' parameters optimization for each value of the pumping power taking into consideration the cross-relaxation and up-conversion processes as well as heating of the active medium. The optimal values of the active medium length, activator concentration and the output mirror reflectivity are determined both for Tm:YAP- and Tm:YAG-laser. The pulse generation of Tm:YAP- and Tm:YAG-lasers is also considered, the parameters of this regime are determined. The comparison shows the suitability of Tm:YAP laser crystal both for cw and pulse generation. The up-conversion influence on the laser characteristics is also analyzed.

PACS 42.60.Gd

1 Introduction

The laser radiation at the wavelength near 2 μm is used in different application fields of technique, particularly, in military engineering [1], meteorology, ranging, altimetry [2] and, especially, in medicine – surgery, ophthalmology, gynaecology, orthopedy, arthroscopy, angioplasty [2, 3]. These applications of 2-μm lasers are stipulated by the strong absorption of this wavelength by water and tissues, on the one hand, and, on the other hand, by the small absorption in the atmosphere and eye-safety as well [3]. The radiation of this wavelength is obtained practically only by lasers based on the active media doped by thulium, holmium or thulium and holmium together [3]. Between them the laser crystal activated by thulium is characterized by the highest differential efficiency in respect to the absorbed pumping radiation [2]. The most widely used crystal matrix for such lasers is yttrium-aluminium garnet $Y_3Al_5O_12$ (YAG). However, some properties, particularly, the higher laser transition cross-section σ_e points out the advisability of yttrium-aluminium perovskite $YAlO_3$ (YAP) as a prospective matrix for thulium laser [4]. The experimental investigations of the Tm:YAP-laser generation in comparison with Tm:YAG-laser [2] show that the differential efficiency of Tm:YAP-laser is twice higher than for the Tm:YAG one. But this investigation was carried out only for some fixed values of laser parameters – geometrical dimensions of active media, activator concentrations, output mirrors reflectivities etc. Here we present results of the Tm:YAP- and Tm:YAG-lasers comparative analysis carried out as optimization problem solving, i.e., by determination of the activator (Tm^{3+}) concentration, the active medium length and the output mirror reflectivity ensuring the highest possible power of laser radiation at the given value of the pumping power and the laser beam divergence.

✉ Fax: +38 032 2742164, E-mail: crystal@polynet.lviv.ua

2 The laser medium characteristics

The yttrium-aluminium perovskite crystal belongs to the space group D_{2h}^{16} and is optically biaxial. The lower symmetry of YAP in comparison with YAG causes the anisotropy of its optical properties and leads to the high polarization of the laser radiation [5]. It may be considered as an advantage of YAP matrix in the case of high harmonics generation. Because of the YAP crystal anisotropy, the influence of the thermo-induced birefringence on the laser beam properties is lower than for the isotropic YAG crystal. The highest amplification in Tm:YAP-laser is achieved for a laser element with axis along the crystallographic direction *b* (installation *Pbnm*) at that the laser radiation is linear polarized and the electric vector is parallel to crystallographic direction *c* [6].

Other advantages of YAP in comparison with YAG are the possibility of the growth rate increasing in 3–5 times without crystal quality decreasing and lower melting temperature for about 70-degrees (2150 K), which is convenient from a technological point of view.

The demerits of YAP include the common tendency for perovskites to twinning and the parasitic growing coloration. However, the technological approaches based on the results of [7, 8] allow one to remove the twinning as well as to minimize the growing coloration by after-growth annealing. Also it must be mentioned that YAP is slightly inferior to YAG in thermomechanical properties; particularly, it has got higher thermal expansion coefficient [9]. For the comparison some parameters of YAP and YAG-crystals are given in Table 1.

In YAP thulium substitutes trivalent yttrium ions in positions with monoclinic symmetry C_s. The optimal values of

Parameter	YAP	YAG	Ref.
Space group	D_{2h}^{16}	O_h^{10}	[6]
Lattice parameters, Å	$a = 5.176$; $b = 5.307$; $c = 7.355$	$a = 12.008$	[6]
Crystallographic position of rare-earth ion (coordination number)	C_s (12)	D_2 (8)	[6]
Melting temperature, K	2150	2220	[9]
Density, g/cm^3	5.36	4.56	[3, 6]
Hardness by Moos	~ 8.5–9	~ 8.25–8.5	[6]
Heat conductivity, W/(cm K)	0.11	0.13	[6]
Specific heat capacity, J/(kg K)	420	588–630	[6]
Thermal expansion, 10^{-6} K^{-1}	9.5 (*a*); 4.3 (*b*); 10.8 (*c*)	7.8–8.5	[3, 9]
Transmission region, μm	0.22–6.5	0.24–6	[6]
Laser breaking point, 10^9 W/cm^2	0.8–1.0	0.8–1.0	[3]
The laser-action wavelength, μm	1.936	2.013	[1, 6]
Refractive index on the laser-action wavelength calculated from Sellmeier formula	1.9048(*a*); 1,9185 (*b*); 1.9270 (*c*)	1.8123	[3]
Stimulated emission effective cross-section at 293 K, 10^{-21} cm^2	5.0	2.2	[5]
The effective absorption cross-section on the laser-action wavelength at 293 K, 10^{-21} cm^2	0.486	0.077	[4]
Pumping wavelength, μm	0.795	0.785	[2]
Absorption cross-section on the pumping wavelength, 10^{-21} cm^2	9.1	6.5	[11, 15]
Absorption coefficient in the crystal transmission region, cm^{-1}	0.005	0.005	[7, 8, 16]
The upper laser level lifetime, ms (at the thulium concentration, at. %)	4.4–4.9 (1) 2.04 (5)	11 (1); 9.1 (10.3)	[4, 16]

TABLE 1 The parameters of YAP and YAG laser crystals

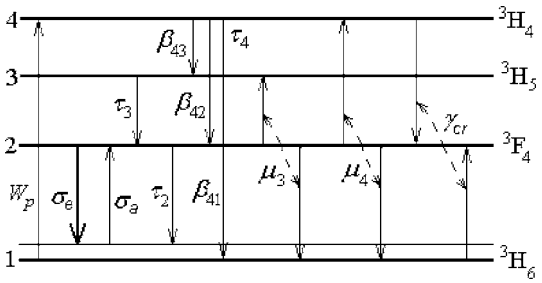

FIGURE 1 Quasi-three-level generation scheme of thulium laser

thulium concentration in YAP are estimated in [2] and is about 3–4 at. %. The structural parameters of Tm:YAP with ~ 4 at. % of thulium are given in [8].

The scheme of thulium laser generation is shown at Fig. 1. The numbering of the energy manifolds indicated here (1...4) are used hereinafter in this paper. The following processes taking place during generation are depicted: pumping to the $^3H_4$ manifold with rate W_p; spontaneous transitions from $^3H_4$, $^3H_5$ and $^3F_4$ manifolds, τ_4, τ_3, τ_2 are their lifetimes, β_{4i}, $i = 1...3$ are the coefficients of luminescence branching; in accordance with [10] we use the values $\beta_{43} = 0.55$ and $\beta_{42} = 0.05$ obtained for Tm:YAG; the cross-relaxation $(^3H_6, {}^3H_4) \rightarrow 2(^3F_4)$ with rate γ_{cr}; the up-conversion processes $(^3F_4, {}^3F_4) \rightarrow (^3H_5, {}^3H_6)$ and $(^3F_4, {}^3F_4) \rightarrow (^3H_4, {}^3H_6)$ with up-conversion parameters μ_3 and μ_4, respectively [10]; laser action on the $^3F_4 \rightarrow {}^3H_6$ transition with the effective cross-section σ_e; the laser radiation absorption between manifolds $^3H_6$ and $^3F_4$ with the effective cross-section σ_a. In accordance with [10], we do not take into account the cross-relaxation $(^3H_5, {}^3H_6) \rightarrow 2(^3F_4)$ because of its sufficiently low rate.

The most effective pumping of Tm:YAG- and Tm:YAP-laser is realized by AlGaAs laser diodes on the wavelength of 0.785 and 0.795 μm, respectively, due to the transition $^3H_6 \rightarrow {}^3H_4$. The laser action of Tm:YAP- and Tm:YAG-lasers takes place on the $^3F_4 \rightarrow {}^3H_6$ transition (Fig. 1) on the wavelengths of 1.936 μm and 2.013 μm, respectively. The lower laser level is one of the 12 Stark sublevels of the ground level [11, 12], so the generation scheme is quasi-three-level.

The pumping efficiency significantly increases due to the cross-relaxation of neighboring thulium ions. The cross-relaxation is effective if the average distance between thulium ions is small enough, i.e., thulium concentration is high. The cross-relaxation rate γ_{cr} dependence on the activator concentration is [13]:

$$\gamma_{cr} = \frac{1}{\tau_4}\left(\frac{N_{Tm}}{N_0}\right)^2, \tag{1}$$

where N_{Tm} is the thulium concentration, N_0 is the thulium concentration at that the cross-relaxation rate is equal to the rate of the thulium ions transitions from $^3H_4$ to the lower manifolds. The data about N_0 and τ_4 values vary in different works, particularly, at thulium concentration 2 at. % it was obtained 0.5; 1.1; 1.6 at. % for N_0 and 0.541; 0.830; 0.510 ms for τ_4 [12, 13]. Here we use the values $N_0 = 0.5$ at. % and $\tau_4 = 0.541$ ms, which were also used for Tm:YAG-laser action consideration in [13] and allow one to obtain the good agreement between theoretical calculations and experimental results. The lifetime of the $^3H_5$ manifold is significantly lower

and equal to 8 μs for Tm:YAG [10]. Because we do not know the value of N_0 for thulium in YAP, all calculations in this work are carried out under the assumption that this parameter is equal for both laser crystals. The $^3H_4$ manifold lifetime for Tm:YAP is very close to the one for Tm:YAG – the theoretical calculation [14] gives 2.5% relative difference between them, so the value of 0.541 ms may be taken as lifetime of the $^3H_4$ manifold for Tm:YAP.

The values of the up-conversion parameters are also known for Tm:YAG crystal only. The up-conversion parameter μ_3 is equal to 3×10^{-18} cm^3/s and the data about μ_4 value differ from 1×10^{-18}–8×10^{-18} cm^3/s for 6% Tm:YAG [10]. Fortunately, this uncertainty has not got a strong influence on our results, because the total up-conversion loss constant μ, determined as a combination (not a summa) of μ_3 and μ_4 [10] depends on μ_3 value firstly. Both up-conversion parameters depend on the thulium concentration as [10]

$$\mu_i = \frac{2U_i}{N_{100\%}} \frac{N_{\mathrm{Tm}}^2}{N_{\mathrm{Tm}}^2 + \tilde{N}^2} = \chi_i \frac{N_{\mathrm{Tm}}^2}{N_{\mathrm{Tm}}^2 + \tilde{N}^2}, \tag{2}$$

where $i = 3, 4$, $\tilde{N}$ is a characteristic dopant concentration, $\tilde{N} = 4.3$ at. % for Tm:YAG, $N_{100\%}$ is a density of available sites in the host material, U_i is a rate of the up-conversion between ions at nearest neighbors positions in the host lattice. The constants χ_3, χ_4 may be determined from the cited above values of up-conversion parameters μ_3, μ_4 of the 6% Tm:YAG. Taking for μ_4 the average value 4.5×10^{-18} cm^3/s, we obtain $\chi_3 = 4.54 \times 10^{-18}$ cm^3/s, $\chi_4 = 6.81 \times 10^{-18}$ cm^3/s. As in the case of the cross-relaxation processes, we use these values for Tm:YAP-laser parameters calculations also.

The important advantage of Tm:YAP-laser crystal is higher transition effective cross-section: $\sigma_e = 5.0 \times 10^{-21}$ cm^2 for Tm:YAP and 2.2×10^{-21} cm^2 for Tm:YAG [4]. Generally, in quasi-three level laser systems the effective laser transition cross-section σ_e is determined by the atomic cross-section σ and the upper laser level Boltzmann factor f_u, $\sigma_e = f_u\sigma$, where $f_u = \frac{1}{Z_u} \exp\left(-\frac{E_u - E_1}{kT}\right)$, $Z_u = \sum_{i=1}^{n_m} \exp\left(-\frac{E_i - E_1}{kT}\right)$ is a partition function, E_i is an energy of the level i in the multiplet, n_m is the number of levels in the multiplet. The absorption cross-section on the laser-action wavelength σ_a is determined as $\sigma_a = f_l\sigma$ where $f_l = \frac{1}{Z_l} \exp\left(-\frac{E_l - E_1}{k_B T}\right)$ is lower laser level Boltzmann factor. The effective cross-sections σ_e and σ_a are connected by the expression [4]:

$$\sigma_e(\nu) = \sigma_a(\nu) \frac{Z_l}{Z_u} \exp\left(\frac{E_{ZL} - h\nu}{k_B T}\right), \tag{3}$$

where ν is a laser radiation frequency, E_{ZL} is zero line energy, i.e., the difference between the energies of the lowest Stark levels of $^3F_4$ and $^3H_6$ manifolds, $E_{ZL} = 0.69$ eV for Tm:YAG and 0.70 eV for Tm:YAP [4]. The values of the effective absorption cross-sections calculated at 20 °C are given in Table 1.

It also must be mentioned, that one of the Tm:YAG active medium advantages is the wide (∼ 400 nm) emission band allows one to realize the tunable lasers [15, 16]. The Tm:YAP crystal may be also used for this application. Particularly, authors of [17] elaborated Tm:YAP-laser with the possibility of wavelength tuning in the region 1.946–1.985 μm.

The absorption cross-section of pumping radiation σ_p for Tm:YAP calculated from the pumping light absorption coefficient [17] is equal to $\sigma_p = 9.1 \times 10^{-21}$ cm^2. The analogous value for Tm:YAG is 6.5×10^{-21} cm^2 [10]. The absorption coefficient α for YAG is ~ 0.005 cm^{-1} in the crystal transmission region [18]; approximately the same estimation may be obtained for YAP crystal from the transmission spectrum given in [7, 8].

For both laser crystals the upper laser level lifetime τ_2 depends on the thulium concentration: for Tm:YAP it is equal to 4.4–4.9 ms at thulium concentrations 1 at. % and 2.04 ms at 5 at. % [19], for Tm:YAG it is equal to 11 ms at 1 at. % and 9.1 ms at 10.3 at. % [4]. Here we approximate the lifetime dependencies on concentration by the expressions similar to (2):

$$\tau_2 = \tau_2^0 \frac{N_{\mathrm{Tm}}^2}{N_{\mathrm{Tm}}^2 + N_\tau^2}. \tag{4}$$

Here $\tau_2^0 = 4.85$ ms, $N_\tau = 4.26$ at. % for Tm:YAP and $\tau_2^0 = 11.02$ ms, $N_\tau = 22.41$ at. % for Tm:YAG.

As seen from the presented data, thulium concentration increasing both in YAP and YAG leads to increasing of the pumping efficiency due to cross-relaxation rate γ_{cr} increasing and, simultaneously, to the upper laser level depletion due to the up-conversion intensification and lifetime decreasing. These two tendencies have got the opposite influence on the laser power, so the thulium optimal concentration value must exist.

3 The thulium microlaser action simulation

3.1 *cw generation*

The effectiveness of thulium lasers on YAP and YAG matrices are compared by collating of the calculated energetic dependencies (the output power on the pumping power) for both crystals. The calculations are based on the system of the rate equations describing the dynamics of the activator levels populations and the laser radiation accumulation in the resonator. This system for quasi-three-level scheme of generation with taking into account the cross-relaxation and up-conversion processes may be written as [10, 11, 13, 20]:

$$\begin{cases} \dfrac{dN_4}{dt} = R + \mu_4 N_2^2 - \dfrac{N_4}{\tau_4} - \gamma_{cr} N_4, \\ \dfrac{dN_3}{dt} = \mu_3 N_2^2 + \beta_{43} \dfrac{N_4}{\tau_4} - \dfrac{N_3}{\tau_3}, \\ \dfrac{dN_2}{dt} = 2\gamma_{cr} N_4 - 2(\mu_3 + \mu_4) N_2^2 + \dfrac{N_3}{\tau_3} + \beta_{42} \dfrac{N_4}{\tau_4} - \dfrac{N_2}{\tau_2} \\ \qquad - \dfrac{c(\sigma_e N_2 - \sigma_a N_1)}{A_e l_a} q, \\ N_{\mathrm{Tm}} = N_1 + N_2 + N_3 + N_4, \\ \dfrac{dq}{dt} = c(\sigma_e N_2 - \sigma_a N_1) q - \dfrac{q}{\tau_c}. \end{cases} \tag{5}$$

Here N_1, N_2, N_3, N_4 are activator ions concentrations on manifolds $^3H_6$, $^3F_4$, $^3H_5$, $^3H_4$ respectively, q is a quantity of photons in resonator, connected with laser output power by expression $P = \frac{h\nu}{t_r} \ln\left(\frac{1}{R_2}\right) q$, $t_r = 2l_a/c$ is a time of photon double passing along the resonator, l_a is a active medium

length, $c = c_0/n$, $c_0 = 3 \times 10^8$ m/s, A_e is a laser mode cross-section, $R = W_p N_1$, $W_p = \frac{P_a}{\pi r_p^2 l_a h \nu_p N_1}$ is a pumping rate, r_p is a pumping beam radius, P_a is a absorbed pumping power connected with pumping power P_i falling into the active medium by expression $P_a = P_i(1 - e^{-2\alpha_p l_a})$, α_p is an absorption coefficient at the pumping wavelength, $\alpha_p = \sigma_p N_{Tm}$, "2" in the exponent is present because the pumping radiation twice passes along resonator due to high reflectivity of the laser output mirror on the pumping wavelength, ν_p is a pumping radiation frequency, τ_c is a lifetime of the photon in the resonator, $\tau_c = l_a/c\gamma$, γ are losses during one passing along the resonator, $\gamma = \gamma_i + 0.5(\gamma_1 + \gamma_2)$, γ_1, γ_2 are losses on the mirrors, $\gamma_1 = -\ln R_1$, $\gamma_2 = -\ln R_2$ (in our calculations $R_1 = 1$, i.e., $\gamma_1 = 0$), γ_i are losses in the active medium, $\gamma_i = \alpha l_a$.

Hereinafter we assume the active medium cross-section filling coefficient $A_e/A = 1$, where $A = \pi r_p^2$, $A_e = \pi \varrho_0^2/4$, ϱ_0 is a laser mode beam waist radius (usually microchip lasers mode is TEM_{00}), i.e., all pumping radiation falls at the region corresponding to the laser mode volume.

All derivations in (5) are equal to zero at the stationary generation, and (5) comes to the system of the algebraic equations that allows one to determine the stationary levels populations and photons quantity in resonator. Taking into account that the concentration of thulium on the $^3H_4$, $^3H_5$ manifolds N_4, N_3 are small, so $N_{Tm} \approx N_1 + N_2$, and the inversion of population for quasi-three-level model is equal to $N = N_2 - fN_1$, where $f = \sigma_a/\sigma_e = f_L/f_U$ [19], we may write this system as:

$$\begin{cases} (1+f)\eta_{QY}R - \dfrac{c\sigma_e(1+f)}{Al_a}Nq - \dfrac{fN_{Tm}+N}{\tau_2} \\ \qquad\qquad - \mu\dfrac{(fN_{Tm}+N)^2}{1+f} = 0\,, \\ \left(\sigma_e c N - \dfrac{1}{\tau_c}\right)q = 0\,. \end{cases} \tag{6}$$

Here we designate $\eta_{QY} = \frac{\beta + 2\gamma_{cr}\tau_4}{1 + 2\gamma_{cr}\tau_4}$ is a quantum yield, $\beta = \beta_{42} + \beta_{43}$, $\mu = \mu_3 + \mu_4(2 - \eta_{QY})$ is a total up-conversion loss constant. Note that only in the case $\eta_{QY} = 1$ the total up-conversion loss constant is a sum of μ_3 and μ_4.

The critical inversion N_c and the laser radiation power P may be obtained from (6) after solving with respect to N and q:

$$N_c = \frac{1}{c\sigma_e\tau_c} = \frac{\gamma}{\sigma_e l_a}\,, \tag{7}$$

$$P = \frac{h\nu}{(1+f)}\frac{\gamma_2}{2\gamma}Al_a\frac{fN_{Tm}+N_c}{\tau_2} \times\left[\frac{(1+f)\eta_{QY}R\tau_2}{fN_{Tm}+N_c} - \frac{\mu\tau_2(fN_{Tm}+N_c)}{1+f} - 1\right]. \tag{8}$$

Taking into account $R(P_i)$ dependence, one may obtain the threshold pumping power P_{thresh} as well as the laser slope efficiency η from (8):

$$P_{thresh} = \frac{h\nu_p A(\gamma + \sigma_a l_a N_{Tm})}{(1 - e^{-2\sigma_p N_{Tm} l_a})\eta_{QY}(\sigma_a + \sigma_e)\tau_2} \times\left[1 + \frac{\mu\tau_2(\gamma + \sigma_a l_a N_{Tm})}{(\sigma_a + \sigma_e)l_a}\right], \tag{9}$$

$$\eta = \eta_{St}\frac{\gamma_2}{2\gamma}(1 - e^{-2\sigma_p N_{Tm} l_a})\eta_{QY}\,, \tag{10}$$

here $\eta_{St} = \nu/\nu_p$ is Stox losses coefficient; both values of P_{thresh} and η are calculated with respect to the pumping power P_i falling into the active medium. As seen from (9) and (10), the expression for the slope efficiency is the same as in the case when the up-conversion processes are absent, $\mu = 0$, whereas the threshold pumping power increases with the up-conversion losses increasing.

As seen from (8), the laser radiation power is a function of the output mirror reflectivity R_2 (or the output mirror losses γ_2), the active medium length l_a, the pumping beam cross-section A and the activator concentration N_{Tm}. The last value is directly contained in (8) and, moreover, determines the cross-relaxation rate γ_{cr}, the total up-conversion loss constant μ and the upper level lifetime τ_2. The estimation of the YAG and YAP matrices effectiveness will be carried out in the following way: for the fixed values of the incident pumping power P_i and the pumping beam cross-section A, we determine values of R_2, l_a and N_{Tm} ensuring the maximum of the laser output power, i.e., we solve the problem of the laser parameters optimization. Such an approach has been used by us in [21] for comparison of the Nd:YAG and Yb:YAG crystals as active media for passively Q-switched lasers. The comparison of different laser crystals effectiveness are realized by confrontation of the highest theoretically achieved values of the laser power determined for each value of the incident pumping power P_i and the cross-section A.

Because the pumping rate $W_p = R/N_1$ is proportional to A^{-1}, it follows from (8) that the laser power increases at pumping beam cross-section A decreasing due to pumping power density rising. However, as it was mentioned above, we assume the pumping and the laser beam radii are always in agreement, so laser beam radius ϱ_0 also decreases with r_p decreasing. It leads to increasing of the laser beam divergence $2\theta = \frac{2\lambda}{\pi\varrho_0 n}$. The typical values of the divergence for the industrial produced microchip lasers are about several mrad. In all calculations below we exactly use the laser beam divergence, not the dimensions of pumping and laser beams, because it is one of laser operating characteristics.

The optimal losses γ corresponding to maximum of (8) may be determined from the condition $dP/d\gamma = 0$. This condition comes to the cubic equation for the output laser power described by (8):

$$\gamma^3 + a_2\gamma^2 + a_0 = 0, \tag{11}$$

where

$$a_2 = \frac{\sigma_e + \sigma_a l_a}{2\mu\tau_2} + \sigma_a l_a N_{Tm} - \frac{1}{2}\left(\gamma_i + \frac{\gamma_1}{2}\right),$$

$$a_0 = \left(\gamma_i + \frac{\gamma_1}{2}\right)\frac{\sigma_a(\sigma_e + \sigma_a)l_a^2 N_{Tm}}{2\mu\tau_2} \times\left(1 + \frac{\sigma_a}{\sigma_e + \sigma_a}\mu\tau_2 N_{Tm} - \frac{\sigma_e + \sigma_a}{\sigma_a}\frac{\eta_{QY}\tau_2}{N_{Tm}}R\right).$$

It may be shown that coefficient $a_0 < 0$ if $P_i > P_{thresh}$ and $a_0 \geq 0$ if $P_i \leq P_{thresh}$. At not very high values of α ($\sim 0.5\,\text{cm}^{-1}$) $a_2 > 0$; so in accordance with Cartesian rule of signs it is

one positive root of (11) exists if $P_i > P_{thresh}$, and no one if $P_i \le P_{thresh}$. If the up-conversion processes may be neglected, $\mu \to 0$, (11) comes to the quadratic one with the positive root in the case $P_i > P_{thresh}$:

$$\gamma_{opt} = \sqrt{2(2\gamma_i+\gamma_l)\frac{P_i(1-e^{-2\sigma_p N_{Tm} l_a})\eta_{QY}(\sigma_e+\sigma_a)\tau_2}{Ah\nu_p}} - \sigma_a N_{Tm} l_a \,. \tag{12}$$

Taking into account that (11) or (12) allows one to determine the optimal output mirror reflectivity $R_2 = \exp(-2\gamma - 2\gamma_i - \gamma_l)$, (8) may be considered as a function of two variables: the thulium concentration N_{Tm} and the active medium length l_a.

As is known, the laser action is accompanied by active medium heating. Its main influence on the quasi-three level thulium lasers parameters is caused by effective cross-sections σ_e and σ_a changing due to changing of the Boltzmann factors f_u and f_l. The main heating sources in Tm:YAG and Tm:YAP lasers are the non-radiative transitions $^3H_5 \to {}^3F_4$, the non-radiative portion of the $^3H_4 \to {}^3H_5$ transitions, the upconversion $2\,{}^3F_4 \to {}^3H_6$, $^3H_5$ at that heating occurs due to the energy disagreement between the levels leads to the phonon generation. The disagreement also takes place at cross-relaxation $^3H_6$, $^3H_4 \to 2\,{}^3F_4$ and upconversion $2\,{}^3F_4 \to {}^3H_6$, $^3H_4$, at that the cross-relaxation is accompanied by origination and the upconversion – by disappearance of phonons.

The power density Q caused by these processes is a function of the appropriate levels occupations and may be written as:

$$Q = \varepsilon_{32}\frac{N_3}{\tau_3} + \varepsilon_{43}\frac{N_4}{\tau_{4nr}} + \varepsilon_{uc3}\mu_3 N_2^2 - \varepsilon_{uc4}\mu_4 N_2^2 + \varepsilon_{cr}\gamma_{cr} N_4 \,, \tag{13}$$

where τ_{4nr} is a non-radiative lifetime of the $^3H_4$ level, $\tau_{4nr} = \tau_4/(1-\eta_4)$, η_4 is a radiative quantum efficiency, $\eta_4 = 0.54$ for Tm:YAG and 0.89 for Tm:YAP [14], so $\tau_{4nr} = 1.176$ ms for Tm:YAG and 4.918 ms for Tm:YAP, ε_{32}, ε_{43} are energies of the $^3H_5 \to {}^3F_4$ and $^3H_4 \to {}^3H_5$ transitions, respectively, $\varepsilon_{32} = 0.26$ eV, $\varepsilon_{43} = 0.46$ eV for Tm:YAG, $\varepsilon_{32} = 0.28$ eV, $\varepsilon_{43} = 0.47$ eV for Tm:YAP, ε_{uc3}, ε_{uc4}, ε_{cr} are energy disagreements in the processes of upconversion $2\,{}^3F_4 \to {}^3H_6$, $^3H_5$, $2\,{}^3F_4 \to {}^3H_6$, $^3H_5$ and cross-relaxation processes $^3H_6$, $^3H_4 \to 2\,{}^3F_4$ respectively, $\varepsilon_{uc3} = 0.182$ eV, $\varepsilon_{uc4} = \varepsilon_{cr} = 0.02$ eV for Tm:YAG and $\varepsilon_{uc3} = 0.24$ eV, $\varepsilon_{uc4} = \varepsilon_{cr} = 0.12$ eV for Tm:YAP.

The concentration N_4 and the relation N_3/τ_3 may be expressed from the two first equations of the system (5): $N_4 = \tau_4 \frac{R+\mu_4 N_2^2}{1+\gamma_{cr}\tau_4}$, $\frac{N_3}{\tau_3} = \mu_3 N_2^2 + \beta_{43}\frac{R+\mu_4 N_2^2}{1+\gamma_{cr}\tau_4}$, where $N_2 \approx \frac{fN_{Tm}+N_c}{1+f}$ is an upper laser level occupation.

When the power density Q is determined from (13), the stationary temperature distribution in the active medium may be defined from the heat conductivity equation. Under the assumption of the cylindrical form of the active element, this equation may be written as:

$$\lambda_T\left(\frac{1}{r}\frac{\partial}{\partial r}\left(r\frac{\partial T}{\partial r}\right) + \frac{\partial^2 T}{\partial z^2}\right) = Q(r) \,, \tag{14}$$

where λ_T is a heat conductivity. Because heating takes place only in the region where the pumping radiation is absorbed, we described the radial distribution of Q as $Q(r) = \begin{cases} Q, & r \le r_p \\ 0, & r > r_p \end{cases}$. The edge conditions for (14) follow from the requirement of the equality of the heat flows from center of the active element to its surface and from the surface to the environment – so called third type edge conditions:

$$-\lambda_T\frac{\partial T}{\partial \boldsymbol{n}} = \alpha_T(T_s - T_e) \,, \tag{15}$$

where $\partial T/\partial \boldsymbol{n}$ is a derivation in the line of normal to the surface, T_s is a surface temperature, T_e is an environment temperature, $T_e = 293$ K, α_T is a heat evolution coefficient. For the systems cooled by the thermal contact with more cool gas environment the heat evolution coefficient $\alpha_T \le 10^{-2}$ W/(s m^2 K) [5]; in our calculations we used the value $\alpha_T = 0.01$ W/(s m^2 K).

The solution of (14) obtained by the integral transformations method [22] is:

$$T(r,z) = T_e + \frac{4Q}{\lambda_T}R_a r_p l_a^2 \times \sum_{i,j=1}^{\infty}\frac{\varrho_i\kappa_j}{\varrho_i^2 l_a^2 + \kappa_j^2 R_a^2}\frac{J_1\left(\varrho_i\frac{r_p}{R_a}\right)\left(\sin\kappa_j + 2\frac{h_l}{\kappa_j}\sin^2\frac{\kappa_j}{2}\right)}{J_0^2(\varrho_i)\left(\varrho_i^2 + h_R^2\right)\left(\kappa_j^2 + h_l^2 + 2h_l\right)} \times J_0\left(\varrho_i\frac{r}{R_a}\right)\left(\cos\left(\kappa_j\frac{z}{l_a}\right) + \frac{h_l}{\kappa_j}\sin\left(\kappa_j\frac{z}{l_a}\right)\right), \tag{16}$$

where $J_0(r)$, $J_1(r)$ are the first kind Bessel functions, R_a is an active element radius, here $R_a = 1.5$ mm (the typical radius of the laser rod), $h_R = \alpha_T R_a/\lambda_T$, $h_l = \alpha_T l_a/\lambda_T$, ϱ_i and κ_i are the roots of the equations $\varrho_i J_1(\varrho_i) = h_R J_0(\varrho_i)$ and $tg\kappa_i = \frac{2h_l\kappa_i}{\kappa_i^2 - h_l^2}$, respectively.

In our calculations we used the temperature on the active element axis ($r = 0$) averaged on the active medium length, $T_{aver} = \frac{1}{l_a}\int_0^{l_a} T(r=0,z)\,dz$ that amounts to

$$T_{aver} = T_e + \frac{4Q}{\lambda_T}R_a r_p l_a^2 \times \sum_{i,j=1}^{\infty}\frac{\varrho_i}{\varrho_i^2 l_a^2 + \kappa_j^2 R_a^2}\frac{J_1\left(\varrho_i\frac{r_p}{R_a}\right)\left(\sin\kappa_j + 2\frac{h_l}{\kappa_j}\sin^2\frac{\kappa_j}{2}\right)^2}{J_0^2(\varrho_i)\left(\varrho_i^2 + h_R^2\right)\left(\kappa_j^2 + h_l^2 + 2h_l\right)} \,. \tag{17}$$

In accordance with (7) the inversion N_c depends on the effective laser cross-section value σ_e and, consequently, on the temperature, but, on the other hand, the power density depends on the inversion N_c (see (13)). Because of this interdependency, the laser parameters calculations are carried out in the following way at given values of N_{Tm} and l_a:

(1) at the given value of the temperature, initially 293 K, the output mirror reflectivity R_2, the inversion N_c and the power density Q are defined;
(2) at the determined value of the power density Q the averaged value of the temperature T_{aver} on the laser element axis is calculated in accordance with (17);
(3) if the difference between the calculated value of the temperature and the previous one is more than 0.01 K, the points (1), (2) are repeated; otherwise the laser parameters,

i.e., the output power, the slope efficiency, the threshold pumping power as well as the pulse regime parameters are calculated.

Obtained by this procedure, typical dependencies of the laser power on the thulium concentration N_{Tm} and the active medium length l_{a} for Tm:YAP and Tm:YAG crystals are shown at Fig. 2 at the pumping power $P_{\mathrm{i}} = 1$ W and the divergence of 2 mrad and at Fig. 3 at the pumping power $P_{\mathrm{i}} = 5$ W and divergence $\theta = 8$ mrad.

As seen from Figs. 2 and 3, the $P(N_{\mathrm{Tm}}, l_{\mathrm{a}})$, these dependencies have got maxima, more well-defined at lower beam divergences θ (Fig. 2). These maxima existence is caused by the fact that activator concentration N_{Tm} raising leads to pumping rate increasing due to cross-relaxation rate γ_{cr} (1) increasing on the one hand, and to upper laser level lifetime τ_2 decreasing and up-conversion losses increasing on the other hand. Active medium length l_{a} increasing leads to the more effective absorption of the pumping radiation and to total active centers quantity increasing, on the one hand, and to pumping power density decreasing as well as to increasing of the losses in the active medium, on the other hand. Thus, the thulium laser parameters optimization consists of the determination of the optimal N_{Tm}, l_{a} and R_2 values for the given values of the incident pumping power P_{i} and divergence θ (or the pumping beam cross-section A).

It must be mentioned that the character of the $P(N_{\mathrm{Tm}}, l_{\mathrm{a}})$ dependencies at higher beam divergences θ indicates lower sensitivity to the activator concentration and active medium length deviation from the optimal values in comparison with $P(N_{\mathrm{Tm}}, l_{\mathrm{a}})$ for lower θ. This peculiarity is more essential for Tm:YAG (Fig. 3b). As seen from this figure, the power decreasing is comparatively small for Tm:YAG-laser in the region of N_{Tm} and l_{a} values higher than optimal ones. It is caused obviously by the weaker upper laser level lifetime dependence on the activator concentration for Tm:YAG.

Here the laser parameters optimization is carried out for the Tm:YAP- and Tm:YAG-lasers comparative analysis. For both lasers the optimal values of N_{Tm}, l_{a}, γ_2 as well as the highest achievable laser power P at fixed values of P_{i} and θ are calculated. The results of the highest achievable output power P calculations at $P_{\mathrm{i}} = 0$–5 W and laser beam divergence $\theta = 2$, 8 mrad are presented at Fig. 4a. The analogous dependencies of the optimal activator concentration N_{Tm}, the optimal active medium length l_{a}, the optimal output mirror reflectivity $R_2 = \exp(-\gamma_2)$, the corresponding slope efficiency η and the threshold pumping power P_{thresh} are shown at Fig. 4b–f.

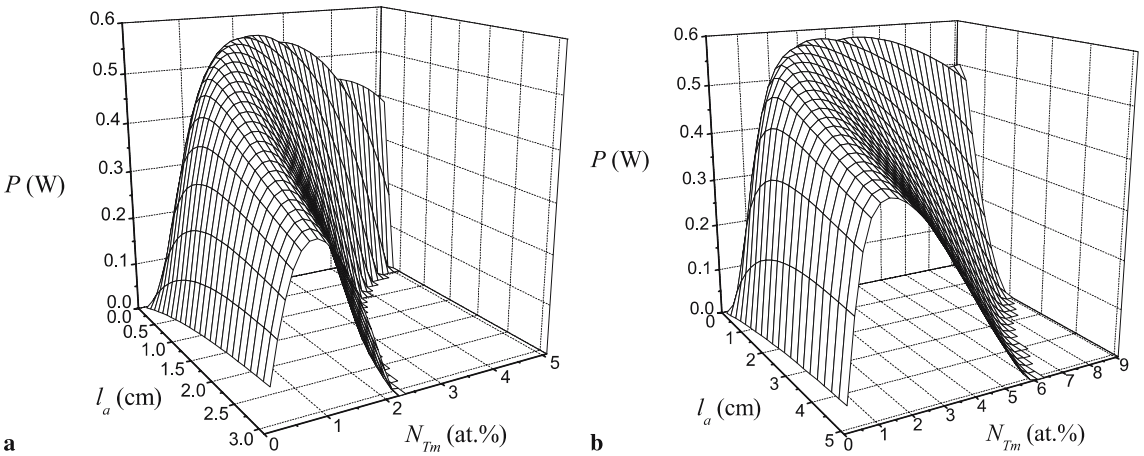

FIGURE 2 The dependencies of the laser power P on the thulium concentration N_{Tm} and active medium length l_{a} at the incident pumping power $P_{\mathrm{i}} = 1$ W and divergence $\theta = 2$ mrad for lasers on Tm:YAP (**a**) and Tm:YAG (**b**)

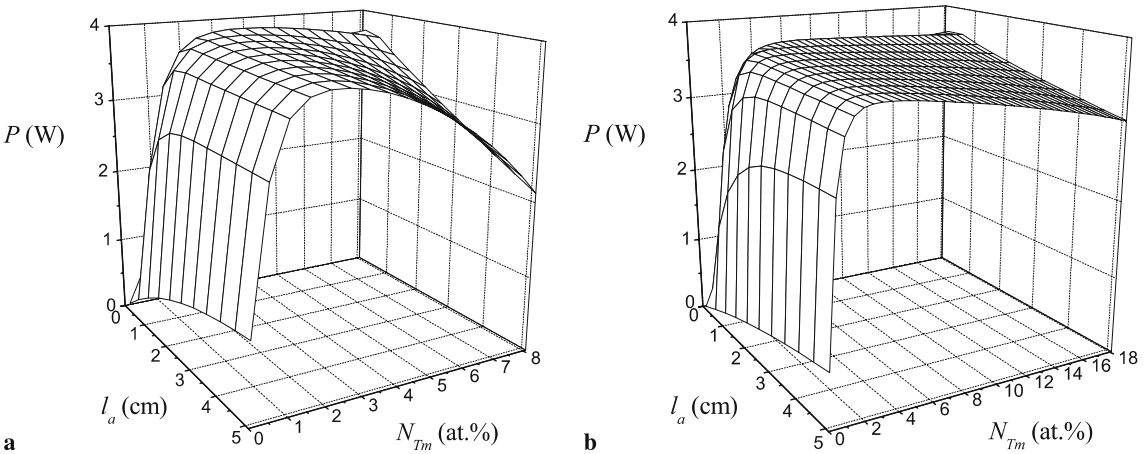

FIGURE 3 The dependencies of the laser power P and on the thulium concentration N_{Tm} and active medium length l_{a} at the incident pumping power $P_{\mathrm{i}} = 5$ W and divergence $\theta = 8$ mrad for lasers on Tm:YAP (**a**) and Tm:YAG (**b**)

As seen from Fig. 4a and e–f, the laser power, the slope efficiency and the threshold pumping power are rather higher for Tm:YAP-laser in comparison with Tm:YAG at the fixed value of the divergence θ. All these values increase with P_i increasing.

The optimal values of the activator concentration N_{Tm} (Fig. 4b) are essentially higher for Tm:YAG-laser (until 10 at. %), whereas for Tm:YAP they are equal to 1–4 at. %. The last values are in agreement with the experimental determination of the optimal activator concentration for Tm:YAP [2]. The optimal active medium length is equal to several millimeters for both lasers. The dependencies of the optimal length l_a on the pumping power have got the different character for low and high divergences: l_a increases with pumping power increasing for the low values of θ and decreases for higher ones. As it follows from our calculations for

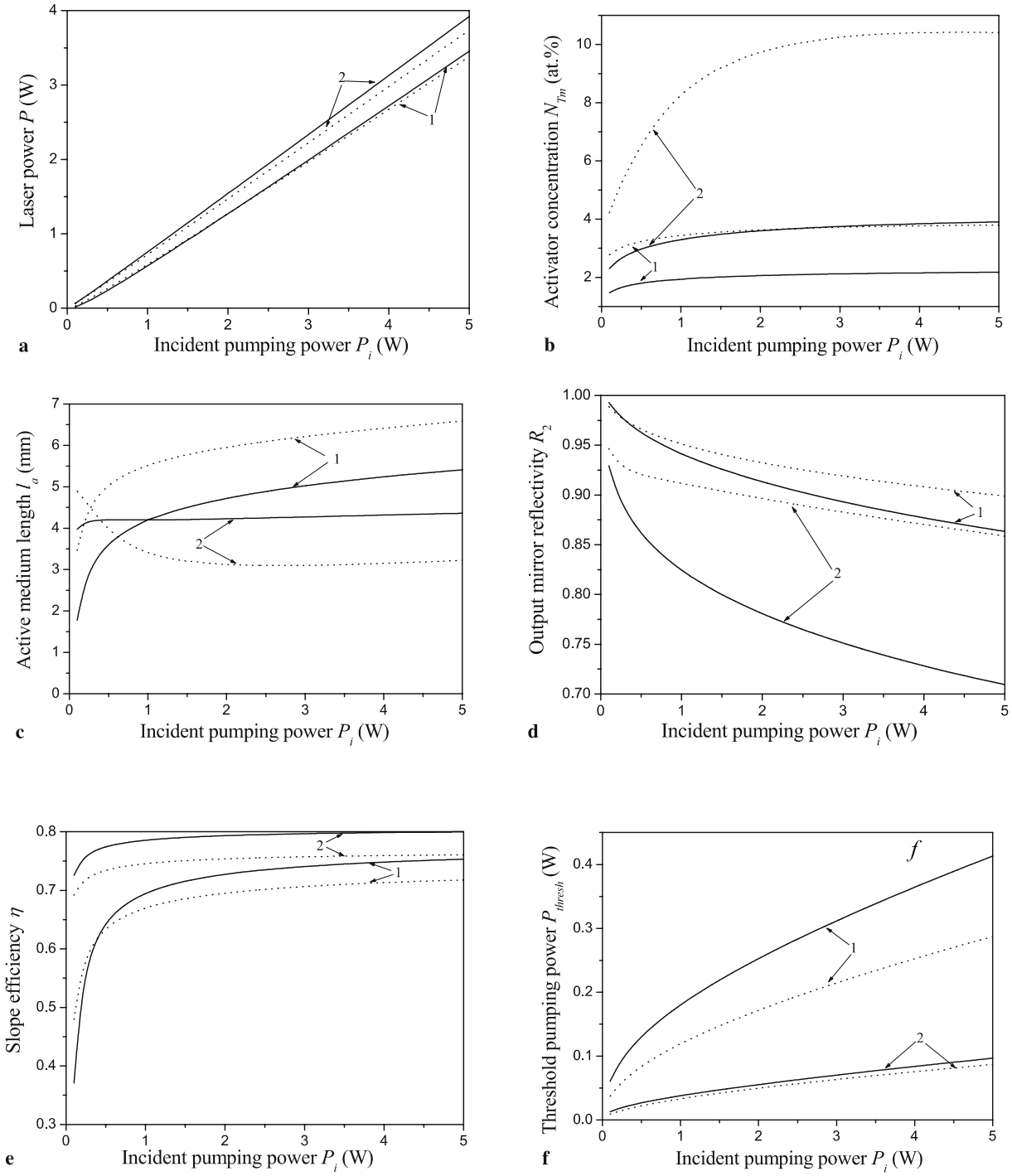

FIGURE 4 The dependencies of the maximum achievable laser power P (**a**), the optimal activator concentration N_{Tm} (**b**), the optimal active medium length l_a (**c**), the optimal output mirror reflectivity R_2 (**d**), the slope efficiency η (**e**) and the threshold pumping power P_{thresh} (**f**) on the incident pumping power P_i at the laser beam divergence $\theta = 2$ (*curves 1*) and 8 mrad (*curves 2*). *Solid curves* are for Tm:YAP-laser, *dashed ones* are for Tm:YAG-laser

other values of θ, at the intermediate values of the laser beam divergence these dependencies have got the non-monotonous character.

The optimal value of the output mirror reflectivity R_2 decreases with pumping power increasing (Fig. 4d) and lies at the given values of P_i and θ in the range of 0.71–0.99 and 0.86–0.99 for Tm:YAP- and Tm:YAG-lasers, respectively.

The dependencies of the averaged temperature of heating T_{aver} (17) on the incident pumping power P_i are approximately linear both for Tm:YAP and Tm:YAG crystals at the P_i values up to 5 W. At that T_{aver} is essentially lower for Tm:YAG-laser: at the incident pumping power P_i about 5 W the difference $T_{aver} - T_e$ is equal to $\sim 25\,^\circ$C, whereas for Tm:YAP this value is about 80 °C. Obviously, it is caused by higher values of the energy disagreement in the upconversion and cross-relaxation processes for Tm:YAP as well as by lower value of the heat conductivity λ_T for this crystal (see Table 1). If heating is not taking into account (in the other words, if the active element is intensively cooled), the values of the laser power obtained after the optimization are insignificantly higher than the presented at Fig. 4a: the relative differences between them do not exceed 4%. The analogous differences between the slope efficiencies η and threshold pumping powers P_{thresh} are also low: the slope efficiencies increase on $\sim 1\%$ and P_{thresh} decrease on 0.3–22% for both laser materials if heating is not taking into account. It must be emphasized that such a low heating influence on the laser power, slope efficiency and threshold pumping power is a consequence of the optimization procedure: in experimental studies the laser parameters (activator concentration, active element length, etc.) are certainly constant, so the observed influence of heating is more essential [2, 23]. Indeed, the optimal activator concentrations in the case of the intensive cooling are significantly higher: up to two times for Tm:YAG and to 30% for Tm:YAP. The corresponding active medium lengths are lower than the ones presented at Fig. 4c: up to two times for Tm:YAG and to 37% for Tm:YAP. The optimal output mirror reflectivities change less significant: they increase up to 7% for both materials.

It must be mentioned that the thulium laser generation analysis was carried out in [1, 13] without up-conversion processes taking into account. On the other hand, it is shown in [10] that the up-conversion losses in Tm:YAG mainly contribute to a higher threshold pumping power P_{thresh} value, particularly, the calculated value of P_{thresh} increases twice in comparison with a case when the up-conversion is not considered for thulium concentration 6 at. %. We also try to determine the influence of the up-conversion on the optimal values of the laser parameters by calculation of the dependencies analogous to the ones presented in Fig. 4a–f at the up-conversion parameters μ_3, μ_4 equal to zero. As it follows from the calculations, the output power obtained after laser parameters optimization slightly increases for both laser materials: in 3–40% for Tm:YAG and 2.5–15% for Tm:YAP. At that the highest relative differences takes place at the low laser beam divergence θ (2 mrad) and low incident pumping power P_i (0.1 W). The relative differences between the optimal slope efficiencies for Tm:YAG are in the limits of 25%, whereas for Tm:YAP they are not higher than 10%. The threshold pumping power changes more significantly: in 1.2–2.5 times for Tm:YAG and up to 30% for Tm:YAP. The optimal values of the activator concentrations N_{Tm} also changes more significant for Tm:YAG: they increase in 2–3.5 times in the case of the up-conversion absence, whereas for Tm:YAP – only in 20–35% for different values of P_i and θ. The optimal active medium length l_a decreases for both materials: in 1.5–3 times for Tm:YAG and in 15–30% for Tm:YAP. The relative differences for the optimal output mirror reflectivity R_2 are negligible at the low values of beam divergence θ and/or incident pumping power P_i. Only at $\theta = 8$ mrad and $P_i = 5$ W they decrease in 25% for Tm:YAG and in 13% for Tm:YAP. Thus, because all relative differences are lower for Tm:YAP active medium, the up-conversion taking into account is less considerable for this laser crystal than for Tm:YAG one. However, as it is mentioned above, the up-conversion constants, as well as the cross-relaxation rate, are known for Tm:YAG only, so the conclusions of the up-conversion influence on the Tm:YAP-laser parameters have got the uncertainty.

For the avoidance of this uncertainty influence on our conclusions, we carried out our calculations for Tm:YAP crystals with cross-relaxation rate γ_{cr} twice lower and, simultaneously, up-conversion parameters μ_3, μ_4 twofold higher than used in the previous calculations. Obviously, it may lead to laser power decreasing as well as to changing of the optimal N_{Tm}, l_a and R_2 values. As it follows from the calculations, the laser power changes insignificantly at the beam divergence 8 mrad – within the limits of 7% and remains higher than the laser power of Tm:YAG. At lower values of beam divergence (2 mrad) this change is higher – up to 40% at the low values of the incident pumping power P_i and 7% at $P_i \sim 5$ W. At that the Tm:YAP laser power becomes lower than the ones of Tm:YAG. At that the slope efficiency η decreases in 5–20% at 2 mrad and in 1–5% at 8 mrad and the threshold pumping power P_{thresh} increases in 7–13% at 2 mrad and in 15–40% at 8 mrad. The optimal values of laser parameters do not change significantly: the activator concentration N_{Tm} and output mirror reflectivity R_2 increase in few percents, whereas the active medium length l_a decreases in 3–15% at both values of laser beam divergence. Because the case of the simultaneous opposite changes of the cross-relaxation rate and the up-conversion parameters is the "worst" in respect to ensuring of the highest laser power, it may be say that these calculations also confirm the Tm:YAP active medium suitability.

3.2 *The peculiarities of the pulse generation*

Several applications of microlaser, particularly, hydro- and atmosphere monitoring by pulse sondage, lithotripsy, medical diagnostics, etc. need pulse laser radiation. The simulation of the laser generation in pulse regime may be realized, in general, by numerical solving of system (5). However, if the pumping pulse duration is significantly higher than the upper laser level lifetime τ_2, the critical inversion N_c and the average pulse power P are determined by (7) and (8) obtained for cw generation. The parameters of the transient state occurring at the beginning of laser pulse generation in the case of the quasi-three-level generation scheme may be obtained from the system (5) in a similar manner as for four-level scheme [20]. At that we assume that the active medium heating is the same as for the case of cw generation. The delay time t_d, i.e., the period for threshold inversion achieving, the char-

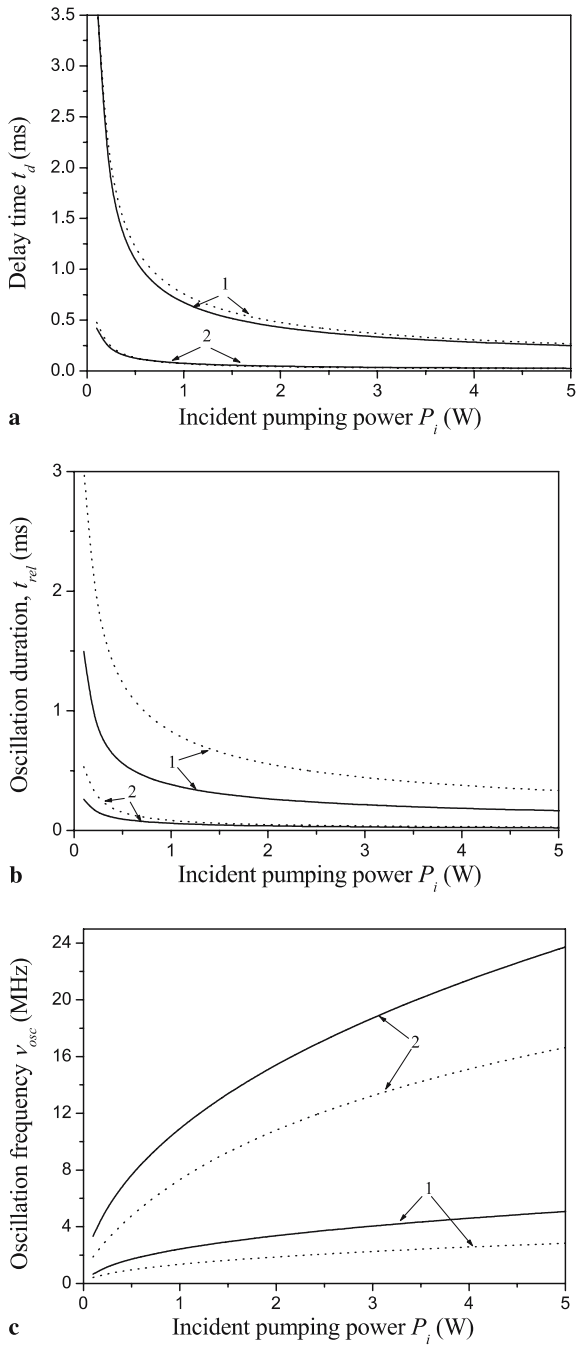

FIGURE 5 The delay time t_d (**a**), the characteristic time of the relaxation oscillation duration t_{rel} (**b**), the oscillation frequency ω (**c**) vs. the pumping power at the laser beam divergence 2 (*curves 1*) and 8 mrad (*curves 2*). *Solid curves* are for Tm:YAP-laser, *dashed ones* are for Tm:YAG-laser

acteristic time of the relaxation oscillation duration t_{rel} and the oscillation frequency ν_{osc} are equal to:

$$t_d = -\frac{\tau_2}{F(\mu)} \times \ln\left(\frac{2(1+f)\tau_2\eta_{QY}R-(1+F(\mu))(fN_{Tm}+N_c)}{2(1+f)\tau_2\eta_{QY}R-(1-F(\mu))(fN_{Tm}+N_c)}\right), \quad (18)$$

$$t_{rel} = 2\left(\frac{\sigma_e(1+f)c}{Al_a}q_0+\frac{1}{\tau_2}+\frac{2}{1+f}\mu(fN_{Tm}+N_c)\right)^{-1}, \quad (19)$$

$$\nu_{osc} = \sqrt{\nu_0^2 - 1/t_{rel}}, \quad (20)$$

where $F(\mu) = \sqrt{1+4\tau_2^2\mu\eta_{QY}R}$, $\nu_0^2 = \frac{\sigma_e^2(1+f)c^2}{Al_a}q_0N_c$, q_0 is a stationary quantity of photons in resonator. We have always got $\nu_{osc} \approx \nu_0$ for the lasers considered in this paper.

The results of the pulse regime parameters calculations in accordance with (18)–(20) are shown at Fig. 5a–c.

As seen from Fig. 5a, the value of the delay time t_d both for Tm:YAP- and Tm:YAG-lasers is about 3.5 ms or lower and decreases with pumping power increasing. The relaxation oscillations duration t_{rel} (Fig. 5b) has got the values close to the ones of t_d and also decreases with pumping power increasing. At that both t_d and t_{rel} are rather lower for Tm:YAP-laser than for Tm:YAG one. The oscillation frequency ν_{osc} is about 1–25 MHz for both lasers and increases with P_i increasing (Fig. 5c), at that for Tm:YAP-laser the frequency is higher. The general character of these dependencies corresponds to the one for the four-level laser [20]. If the up-conversion is not taking into consideration, the values of the delay time t_d and the oscillations duration t_{rel} are practically not changed in the case of Tm:YAP and become 50% lower for Tm:YAG at $\theta = 2$ mrad and 2.5 times higher for $\theta = 8$ mrad and $P_i \sim 5$ W. The oscillation frequency ν_{osc} is higher both for Tm:YAG and Tm:YAP laser crystals: the relative differences are equal to 28–90% for Tm:YAG and 12–15% for Tm:YAP.

To avoid the uncertainty of the cross-relaxation rate γ_{cr} and up-conversion parameters μ_3, μ_4 influence on the presented results for Tm:YAP, the calculations are also carried out at the values of γ_{cr}, μ_3, μ_4 varied in the same manner as in the previous section of this paper. At that the value of the delay time t_d changes in the limits of 15%, and at the different values of P_i and θ it may be higher or lower than the one presented at Fig. 5a. The relaxation oscillations duration t_{rel} decreases in comparison with the one presented at Fig. 5b in 1–37%. The oscillation frequency ν_{osc} decreases at $\theta = 2$ mrad in 1.5–8% and increases at $\theta = 8$ mrad in 1–3.5%.

If the laser active element is intensively cooled and its temperature is close to 20 °C, the delay time t_d and the oscillations duration t_{rel} are lower than the ones presented at Fig. 5a and b: the relative differences are up to 30–90% for both laser materials at the different values of the pumping power and the laser beam divergence. The oscillation frequency ν_{osc} increase for both materials at the presence of intensive cooling: in 1–55% for Tm:YAG and 1–22% for Tm:YAP. Thus cooling may noticeably improve the dynamical characteristics of Tm:YAG- and Tm:YAP-lasers due to delay time and oscillations duration shortening.

The estimation of the power splash at laser pulse beginning is carried out by numerical solving of (5) by the forth-order Runge–Kutta technique. It indicates the significant splash: its relative value P_{max}/P, where P_{max} is the power in the splash, is about 40–50 and slightly depends on the parameters of pumping for both lasers.

Thus the Tm:YAP laser crystal has got slight advantage in the case of the pulse generation due to its better dynamical characteristics, namely lower t_d and t_{rel} values.

As known, the short pulse ($\sim$ 1–10 ns) laser operation may be also achieved due to Q-switching. Active Q-switching of Tm:YAG or Tm,Cr:YAG laser may be realized by elec-

trooptical or acousto–optical [24] modulators. Cr^{2+}:ZnSe crystal may be used as a passive Q-switch for Tm:YAG laser [25]. As known from the theory of Q-switching [19] the energy of the Q-switched laser pulse is proportional to the inversion N_{i} achieved before the generation beginning. The maximal value of the inversion $N_{\mathrm{i\,max}}$ obtained at fixed pumping rate R determined from (5) at $q = 0$ is $N_{\mathrm{i\,max}} = \frac{1+f}{2\mu\tau_2}\left(\sqrt{1+4\tau_2^2\mu\eta_{\mathrm{QY}}R}-1\right) - fN_{\mathrm{Tm}}$. The derivatives $\partial N_{\mathrm{i\,max}}/\partial\tau_2$ and $\partial N_{\mathrm{i\,max}}/\partial\mu$ are positive, so the active media with higher lifetimes of the upper laser level τ_2 and higher up-conversion loss constant μ allow one to obtain higher inversion and higher energies in the pulse as a result. Because of higher values of τ_2, Tm:YAG crystal might be more perspective for Q-switching than Tm:YAP. The detail analysis of the Q-switching operation is beyond the bounds of this paper and is intended in future.

4 Conclusions

We considered the micro lasers based on the yttrium-aluminium perovskite and yttrium-aluminium garnet doped with thulium used as a coherent light sources in the 2 μm wavelength range. The comparative analysis of these lasers is carried out by means of the lasers parameters optimization for each value of the incident pumping power. As shown, under the assumption that the cross-relaxation rate and the up-conversion parameters for Tm:YAG and Tm:YAP are close, at the same values of the incident pumping power and the laser beam divergence the maximal achieved laser power is higher for Tm:YAP-laser in comparison with Tm:YAG.

The optimal active medium length for both lasers is about 2–7 mm at the incident pumping power ≤ 5 W, and the optimal values of the activator concentration is about $\sim$ 1–4 at. % for Tm:YAP and until 10 at.or Tm:YAG. The optimal value of the output mirror reflectivity R_2 lies in the range of 0.71–0.99 and 0.86–0.99 for Tm:YAP- and Tm:YAG-lasers, respectively.

The pulse generation of Tm:YAP and Tm:YAG-lasers is also considered. As shown, the typical value of the delay time and the relaxation oscillation duration for both lasers is in the limits of 3.5 ms, and the oscillation frequency is about 1–25 MHz. The delay time and the relaxation oscillation duration are lower, and the oscillations frequency is higher for Tm:YAP active medium in comparison with Tm:YAG, that indicates Tm:YAP crystal rather more suitable for the pulse generation. The relative value of the power splash at the beginning of the laser pulse for both lasers is equal to 40–50 and slightly depends on the parameters of pumping.

The estimation of the up-conversion processes influence on the optimal laser parameters is carried out by comparison of the results obtained for the cases when the up-conversion is taking into account and when it is neglected. As follows from our calculations, the output power obtained after laser parameters optimization slightly increases for both laser materials: in 3–40% for Tm:YAG and 2.5–15% for Tm:YAP. the value of output power obtained after laser parameters optimization is not sensitive to the presence of the up-conversion processes. The relative difference of the slope efficiency for both cases is also not high: $\leq 25\%$ for Tm:YAG and $\leq 10\%$ for Tm:YAP. The threshold pumping power is significantly lower – in 1.2–2.5 times for Tm:YAG and up to 30% for Tm:YAP. The optimal values of the activator concentrations and the active medium length are different in both cases: the relative differences for these values are about 1.5–3 times for Tm:YAG and 15–35% for Tm:YAP. The optimal output mirror reflectivity is lower if the up-conversion is absent, as well as the values of the delay time and oscillation duration are higher.

Thus, our calculations show that Tm:YAP active medium is more perspective for cw generation in comparison with Tm:YAG one because it allows one to obtain comparative or higher output power at the reasonable activator concentrations and, at the same time, has got smaller value of the depolarization losses and higher manufacturability. Also the Tm:YAP crystal has got some advantage in the case of the short pulse generation because of smaller delay time and relaxation oscillation duration. However, both these values for Tm:YAG and Tm:YAP crystals is sufficiently close, so this advantage does not look very significant.

REFERENCES

1 C. Li, J. Song, D. Shen, N.S. Kim, K.-I. Ueda, Opt. Express **4**, 12 (1999)
2 I.F. Elder, M.J.P. Payne, Opt. Commun. **148**, 265 (1998)
3 A.O. Matkovskyy, *The Materials of Quantum Electronics* (Liga-Press, Lviv, 2000) [in Ukrainian]
4 S.A. Payne, L.L. Chase, L.K. Smith, W.L. Kway, W.F. Krupke, IEEE J. Quantum Electron. **QE-28**, 2619 (1992)
5 A.V. Mezenov, L.N. Soms, A.I. Stepanov, *The Solid State Lasers Thermooptics* (Mashinostroenie, Leningrad, 1986) [in Russian]
6 A.A. Kaminskyy, *Laser Crystals* (Springer, New York Heidelberg Berlin, 1981)
7 D. Sugak, A. Durigin, A. Matkovskyy, A. Suchocki, I. Solskii, D. Savitskii, Y.D. Zhydachevskii, F. Wallrafen, K. Kopczynski, Cryst. Res. Technol. **36**, 1223 (2001)
8 A.O. Matkovskii, D.I. Savytskii, D.Y. Sugak, I.M. Solskii, L.O. Vasylechko, Y.D. Zhydachevskii, M. Mond, K. Petermann, F. Wallrafen, J. Cryst. Growth **241**, 455 (2002)
9 F. Gan, *Laser Materials* (World Scientific, Singapore, New Jersey, London, Hong Kong, 1995)
10 G. Rustad, K. Stenersen, IEEE J. Quantum Electron. **QE-32**, 1645 (1996)
11 G. Armagan, A.M. Buoncristiani, W.C. Edwards, A.T. Inge, B. DiBartolo, OSA Proc. Adv. Solid State Lasers, Vol. 6, ed. by H.P. Jenssen, G. Dub (1990)
12 J.M. O'Hare, V.L. Donlan, Phys. Rev. B **14**, 3732 (1976)
13 E.C. Honea, R.J. Beach, S.B. Sutton, J.A. Speth, S.C. Mitchell, J.A. Skidmore, M.A. Emanuel, S.A. Payne, IEEE J. Quantum Electron. **QE-33**, 1592 (1997)
14 J.A. Caird, L.G. DeShazer, J. Nella, IEEE J. Quantum Electron. **QE-11**, 874 (1975)
15 R.C. Stoeman, L. Esterowitz, Opt. Lett. **15**, 486 (1990)
16 G. Quehl, J. Grunert, V. Elman, A. Hemmerich, Opt. Commun. **190**, 303 (2001)
17 N.I. Borodin, P.V. Kriukov, A.V. Popov, S.N. Ushakov, A.V. Shestakov, Quantum Electron. **35**, 511 (2005) [in Russian]
18 G.M. Zverev, Y.D. Goliaev, E.A. Shalaev, A.A. Shokin, *Lasers on the Yttrium-Aliminium Garnet with Neodimium* (Radio i sviaz, Moscow, 1985) [in Russian]
19 H. Manaa, V. Wiedman, R. Moncorge, M. Koselja, J.C. Souriau, J. Phys. IV **4**, 525 (1994)
20 O. Svelto, *Principles of Lasers* (Plenum Press, New York, 1998)
21 O.A. Buryy, S.B. Ubiszkii, S.S. Melnyk, A.O. Matkovskii, Appl. Phys. B **78**, 291 (2004)
22 A.V. Likov, *Heat-mass Exchange. Reference Book* (Energia, Moscow, 1978) [in Russian]
23 T. Thevar, N.P. Barnes, Appl. Opt. **45**, 3352 (2006)
24 L. Esterowitz, R.C. Stoneman, U.S. Patent 4,965,803 (1990)
25 M. Mond, Dissertation (Hamburg University, 2003)